Am J Physiol Heart Circ Physiol 282: H1915–H1923, 2002.
First published January 24, 2002; 10.1152/ajpheart.00867.2001.

Action potential duration restitution and ventricular fibrillation due to rapid focal excitation

MOSHE SWISSA,[1*] ZHILIN QU,[2*] TOSHIHIKO OHARA,[1] MOON-HYOUNG LEE,[1]
SHIEN-FONG LIN,[3] ALAN GARFINKEL,[2] HRAYR S. KARAGUEUZIAN,[1]
JAMES N. WEISS,[2] AND PENG-SHENG CHEN[1]
[1]*Division of Cardiology, Department of Medicine, Cedars-Sinai Medical Center, Los Angeles 90048;*
[2]*Division of Cardiology, Departments of Medicine and Physiology and Physiological Science, University of California at Los Angeles School of Medicine, Los Angeles, California 90095;*
and [3]*Department of Physics and Astronomy, Vanderbilt University, Nashville, Tennessee 37235*

Received 1 October 2001; accepted in final form 21 January 2002

Swissa, Moshe, Zhilin Qu, Toshihiko Ohara, Moon-Hyoung Lee, Shien-Fong Lin, Alan Garfinkel, Hrayr S. Karagueuzian, James N. Weiss, and Peng-Sheng Chen. Action potential duration restitution and ventricular fibrillation due to rapid focal excitation. *Am J Physiol Heart Circ Physiol* 282: H1915–H1923, 2002. First published January 24, 2002; 10.1152/ajpheart.00867.2001.—The focal source hypothesis of ventricular fibrillation (VF) posits that rapid activation from a focal source, rather than action potential duration (APD) restitution properties, is responsible for the maintenance of VF. We injected aconitine (100 μg) into normal isolated perfused swine right ventricles (RVs) stained with 4-{β-[2-(di-*n*-butylamino)-6-naphthyl]vinyl}pyridinium (di-4-ANEPPS) for optical mapping studies. Within 97 ± 163 s, aconitine induced ventricular tachycardia (VT) with a mean cycle length 268 ± 37 ms, which accelerated before converting to VF. Drugs that flatten the APD restitution slope, including diacetyl monoxime (10–20 mM, $n = 6$), bretylium (10–20 μg/ml, $n = 3$), and verapamil (2–4 μg/ml, $n = 3$), reversibly converted VF to VT in all cases. In two RVs, VF persisted despite of the excision of the aconitine site. Simulations in two-dimensional cardiac tissue showed that once VF was initiated, it remained sustained even after the "aconitine" site was eliminated. In this model of focal source VF, the VT-to-VF transition occurred due to a wave break outside the aconitine site, and drugs that flattened the APD restitution slope converted VF to VT despite continuous activation from aconitine site.

arrhythmia; mapping; pacing; tachyarrhythmias

THE MECHANISM OF ventricular fibrillation (VF) is unclear. The multiple wavelet hypothesis (13) posits that dispersion of refractoriness underlies the mechanisms of wave breaks, resulting in the maintenance of VF. The dispersion of refractoriness could be caused either by preexisting electrophysiological or anatomic heterogeneity, or dynamically by steep action potential (AP) duration (APD) restitution (3, 5, 15, 18, 19, 22). Flattening of the APD restitution curve with verapamil, diacetyl monoxime (DAM) (19), and bretylium (3) has been shown to convert VF to a periodic rhythm, or ventricular tachycardia (VT), in canine and porcine ventricles. An alternative hypothesis of cardiac fibrillation is the focal source hypothesis. A rapidly firing focal source induced by aconitine (16) or a mother rotor (4) could drive the entire atria or ventricle into fibrillation. The period of the mother rotor determines the dominant frequency (DF) of cardiac fibrillation. Samie et al. (20) tested the mother rotor hypothesis in rabbit ventricles. They also found that verapamil converted VF to VT, but attributed this to the effect of verapamil on the core size and the period of mother rotor rather than APD restitution. However, because verapamil also flattens APD restitution (19), it is not possible to completely rule out that the antifibrillatory action of verapamil is due to its effects on APD restitution. To resolve this issue, it is necessary to develop an animal model in which VF is caused by rapid focal discharge from a fixed and known location. If drugs that flatten APD restitution convert VF to VT independent of the period of the focal source in this model, then the importance of restitution can be ascertained. For electrical stimulation to achieve 1:1 capture at a period of a rotor (>10 Hz) (20), it usually requires a strong stimulus strength that might exceed 10 mA (1, 6). Because it is unlikely for a mother rotor to generate a 10-mA current, we propose that rapid pacing is not an appropriate model to test the focal source hypothesis of VF. Aconitine, a sodium channel opener that is known to cause focal atrial fibrillation (16), may result in rapid focal discharge from the myocardium at rate approaching 10 Hz. Therefore, we first examined whether direct aconitine injection into the swine right ventricle (RV) would mimic focal source VF. We then studied the effects of verapamil, DAM, and bretylium, which, although they have divergent effects on rotor period and VF cycle length (CL), all flatten the APD restitution.

*M. Swissa and Z. Qu contributed equally to this study.

Address for reprint requests and other correspondence: P.-S. Chen, Rm. 5342, Cedars-Sinai Medical Center, 8700 Beverly Blvd., Los Angeles, CA 90048 (E-mail: chenp@cshs.org).

The costs of publication of this article were defrayed in part by the payment of page charges. The article must therefore be hereby marked "*advertisement*" in accordance with 18 U.S.C. Section 1734 solely to indicate this fact.

METHODS

Tissue preparation. The animal research protocol was approved by the Institutional Animal Care and Use Committee and conformed to the guidelines of the American Heart Association. Eleven farm pigs (25–35 kg wt) of either sex were anesthetized with pentobarbital sodium (20 mg/kg iv). The RVs were isolated and perfused through the right coronary artery with oxygenated Tyrode's solution at 37°C (7). The composition of Tyrode's solution (in mmol/l) was as follows: 125 NaCl, 4.5 KCl, 1.8 NaH_2PO_4, 24 $NaHCO_3$, 2.7 $CaCl_2$, 0.5 $MgCl_2$, and 5.5 dextrose (8). The RVs were placed with the endocardial side down in a tissue bath. VF, which always occurred during heart excision, continued in isolated RVs. After baseline recordings, the tissue was defibrillated and paced at fixed CL of 400 ms with twice the diastolic threshold current and 5-ms pulse width through a bipolar electrode on the epicardial surface.

Pseudo-electrocardiograms (ECG) were recorded via two electrodes on opposing sides of the RV (7). Bipolar electrode pairs were placed at the aconitine injection site and at a site distant from that area.

Optical mapping. The methods of optical mapping was similar to that published previously (10, 21). The isolated RVs were stained for 20 min with the voltage-sensitive dye 4-{β-[2-(di-*n*-butylamino)-6-naphthyl]vinyl}pyridinium (di-4-ANEPPS) (Molecular Probes) in the perfusate and excited with a laser at 532 nm. Light was collected using an image-intensified charge-coupled device camera (Dalsa). The data were gathered at a 2.3-ms sampling interval, acquiring from 128 × 128 sites simultaneously over a 3 × 3-cm^2 area. The duration of each recording was 2.3 s. Data for each pixel were represented on a gray scale, with white representing fully depolarized and black representing fully repolarized states, respectively. Depolarization wave fronts are shown by red lines and repolarization wave backs are shown by blue lines, with their junctions representing wave breaks.

We also manually determined the APD restitution curves by using optical signals recorded during VT, VT-to-VF transition, and VF. On each tracing, a horizontal line was drawn at one-sixth of the maximum AP amplitude from the baseline. The intersection between this line and the upslope of the AP is the time of depolarization, and the intersection between this line and the downslope of the AP is the time of repolarization. The APD and depolarization interval (DI) were defined as the time interval between depolarization and repolarization and between repolarization and depolarization, respectively. The relationship between the APD and the preceding DI was plotted and the APD restitution slopes were calculated by single-exponential fits to the data.

Study protocol. Aconitine (100 μg) was injected locally at the center of the RV, inducing VT and VF. After data acquisition, 10–20 mM DAM ($n = 6$) (19) was infused to convert VF back to VT and then washed out to convert VT back to VF. In three more RVs, we first infused and then washed out bretylium (10–20 μG/ml) ($n = 3$) (3), followed by 2–4 μG/ml verapamil (20) infusion and washout. In one of these three RVs, bretylium was reinfused a second time, followed by reinjection of aconitine and infusion of verapamil with bretylium still present. In two additional RVs, we excised the aconitine site to determine whether VF persisted. Other than DAM and verapamil, we did not use electromechanical uncouplers in the study.

DF analysis. Fast Fourier transform (FFT) was applied to the optical signals at each pixel (1,000 data points for 2.3-s recording) and to the pseudo-ECG and bipolar recordings near and far from aconitine site (50,000 data points for 10-s recording). The frequency corresponding to the largest spectral peak was defined as the DF. The value of DF of each pixel was used to generate an iso-DF map.

Statistical analyses. Student's *t*-tests were used for statistical comparison. $P \leq 0.05$ was considered significant. Analysis of variance with Dunn's (Bonferroni) correction was used to compare the means of three groups. All data are presented as means ± SD.

Computer simulation. Numerical simulations were carried out using the following cable equation (17)

$$C_m \frac{\partial V}{\partial t} = -I_{ion} + \frac{1}{\rho_x S_v}\frac{\partial^2 V}{\partial x^2} + \frac{1}{\rho_y S_v}\frac{\partial^2 V}{\partial y^2} \quad (1)$$

where the membrane capacitance $C_m = 1$ μF/cm^2, the surface-to-volume ratio $S_v = 2{,}000$ cm^{-1}, the transverse and longitudinal resistivities $\rho_x = \rho_y = 0.5$ kΩ·cm, V is voltage, and t is time. We simulated a 10 × 10-cm tissue with "no-flux" boundary conditions. In *Eq. 1*, the ionic current I_{ion} was taken from the Luo-Rudy AP model (12), modified to change AP restitution properties, as specified in the figure legends. We introduced heterogeneity into the tissue by two methods. In the first, we changed the maximum potassium channel conductance ($\bar{G}_K$) through space as follows

$$\bar{G}_K(x,y) = \begin{cases} \alpha\bar{G}_K, & \text{if } x < 5 \text{ cm} \\ [\alpha - \beta(x-5)]\bar{G}_K, & \text{if } 5 \text{ cm} < x < 6 \text{ cm} \\ (\alpha - \beta)\bar{G}_K & \text{if } x > 6 \text{ cm} \end{cases} \quad (2)$$

where $\bar{G}_K = 0.282$ mS/cm^2 and α and β are constants that control the inhomogeneity. In the second, we changed the maximum potassium channel conductance as follows

$$\bar{G}_K(x,y) = \begin{cases} [\alpha + \beta(r-1)]\bar{G}_K \text{ if } r < 1 \text{ cm} \\ \alpha\bar{G}_K, \text{ otherwise} \end{cases} \quad (3)$$

where r is the distance from the aconitine site. We mimicked aconitine-induced automaticity by pacing the tissue at a small area whenever the diastolic interval exceeded a critical (adjustable) value. A pseudo-ECG was constructed by summing membrane voltage, as described previously (23).

RESULTS

Induction of VT and VF by aconitine. In all RV tissues, local injection of aconitine (100 μg) induced VT within 97 ± 162 s. The initial CL was 268 ± 37 ms, which progressively decreased to 156 ± 40 ms before deteriorating to VF. Time from VT induction to VF averaged 377 ± 657 s. Figure 1 shows a typical example. Twenty-five seconds after aconitine injection, the first beat of VT occurred, and pacing was turned off. Figure 1*B* shows a 3-s recording at the onset of VT. The first four beats were paced at a CL of 400 ms and the fifth beat (arrow) occurred before the pacing stimulus. This fifth beat was therefore the first beat of VT with an initial CL of 300 ms. At *time 50 s* (Fig. 1*C*), the VT CL decreased to 150 ms. At *time 76 s* (Fig. 1*D*), the pseudo-ECG recording and the bipolar recording distant from the aconitine site showed VF. However, the aconitine site was still activated at a regular CL of 125 ms. At *time 86 s* (Fig. 1*E*), the aconitine injection site also demonstrated VF. Optical mapping during aconitine-induced VT (Fig. 2*A*) revealed focal activation originating from the aconitine injection site (yellow arrowhead) at 244-ms CL. The wave front first spread

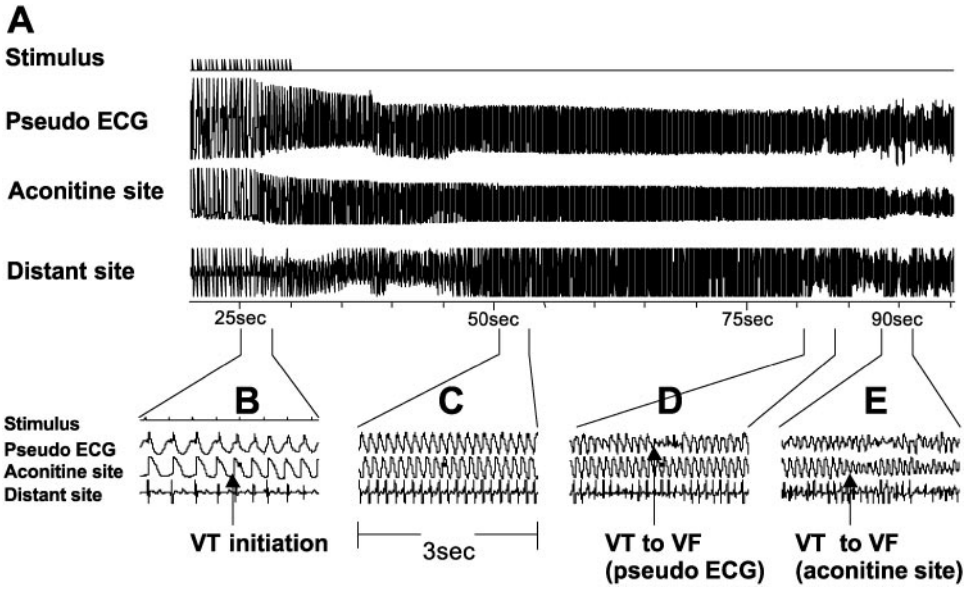

Fig. 1. Example of the aconitine-induced ventricular tachycardia (VT)-to-ventricular fibrillation (VF) ratio (VT to VF). Pseudoelectrocardiogram (ECG) was recorded from electrodes placed on opposite ends of the right ventricle (RV). Time of aconitine injection is *time 0*. *A*: tissue was constantly paced at a 400-ms cycle length (CL) until the induction of VT. *B*: 25 s after injection, VT occurred (arrow) at an initial CL of 300 ms. *C*: 50 s after injection, the VT CL decreased to 150 ms. *D*: conversion of VT to VF (arrow) at *time 76 s*. *E*: activations registered during VF 90 s after aconitine injection.

along the fiber orientation and then to the rest of the tissue, giving rise to the periodic optical potential recordings.

In two episodes, we successfully mapped the transition of VT to VF. Figure 2 shows a 2.3-s recording containing the VT-to-VF transition. The transition occurred when wave breaks were created (Fig. 2*A*, 442-ms panel). Once established, VF was characterized by clockwise and counterclockwise rotating spiral waves, multiple wave breaks, and multiple irregular

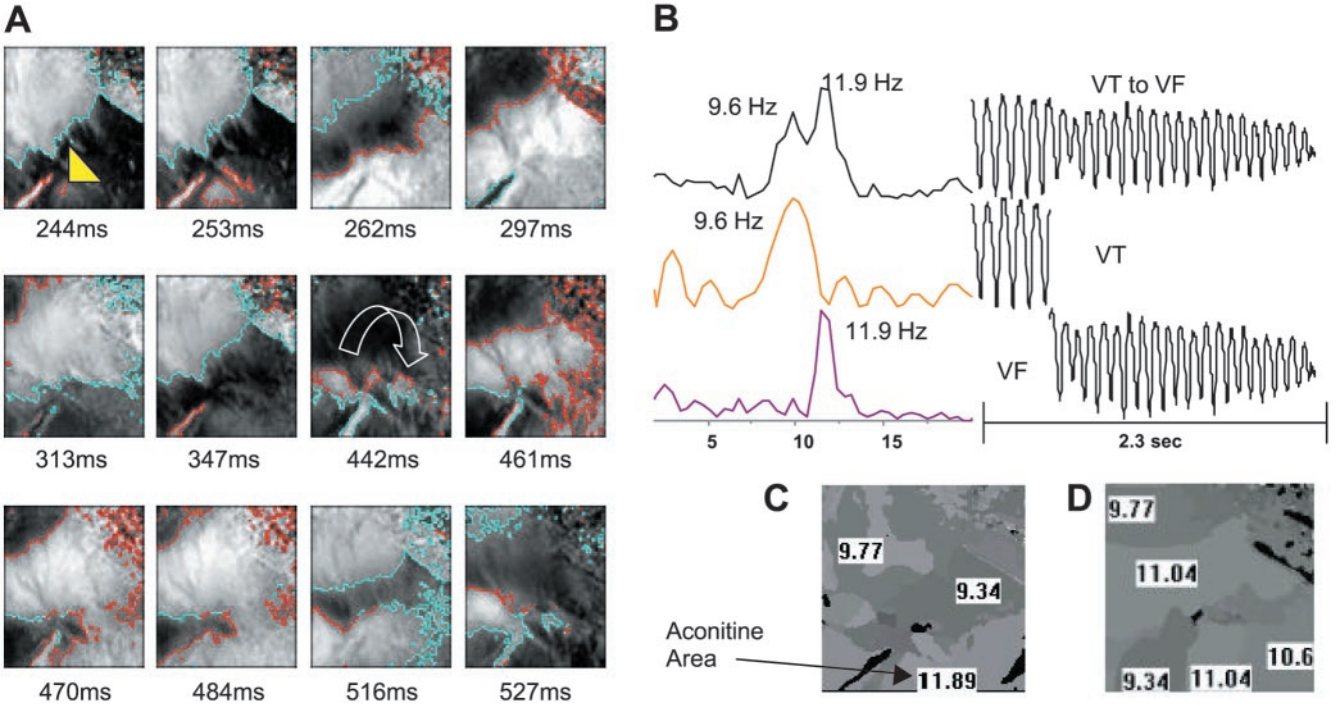

Fig. 2. Aconitine-induced VT-to-VF transition. *A*: 2.3-s recording containing the VT-to-VF transition. The first 6 photos show VT activation. The pattern was characterized by focal activation arising from the aconitine site (arrowhead). The activation first spread along the fiber orientation and then activates the rest tissue. The next 6 photos show a wave break (at 442 ms), followed by clockwise rotating reentrant excitation wave. *B*: fast Fourier transform (FFT) analysis of optical signals at the aconitine site over the full 2.3-s segment revealed two peaks with frequencies of 9.6 and 11.9 Hz. When the FFT analysis was applied to the VT segment alone, only the 9.6-Hz frequency was observed, whereas for the VF segment, only the 11.9-Hz frequency was present. *C*: the isodominant frequency (DF) map shows the distribution of DF, with white color indicating the highest DF and black color indicating the lowest DF. The highest DF in this episode appeared at the aconitine injection site. *D*: shows iso-DF map after excision of aconitine site. More than one region showed high DF.

wave fronts. In Fig. 2*B*, FFT analysis of optical signals at the aconitine site over the full 2.3-s segment revealed two peaks with frequencies of 9.6 and 11.9 Hz. When the FFT analysis was applied to the VT segment alone, only the 9.6-Hz frequency was observed, whereas for the VF segment, only the 11.9-Hz frequency was present. This finding indicates that the frequency changed abruptly at the aconitine site when VF occurred. This was not due to a sudden increase in the automatic focus CL at the aconitine site, because aconitine-induced automaticity accelerated gradually, never abruptly. In addition, the spatial distribution of the DF in the FFT spectra for the whole 2.3-s episode (Fig. 2*C*) illustrates that the low and high frequency originated from different areas and that the maximal frequency was in the aconitine area (11.89 Hz). After the aconitine site was ablated, the maximum DF during VF might not be close to the ablated site (Fig. 2*D*).

Restitution during VT, VT-to-VF transition, and VF. An example of optical recording of aconitine-induced VT during VT-to-VF transition and during VF are given in Fig. 3*A*. The APD restitution curves of these three different phases are shown in Fig. 3*B*. The maximal slopes of the APD restitution curves were 0.226, 3.3, and 1.76 for VT, VT-to-VF transition, and VF, respectively.

Conversion of VF to VT by flattening restitution. DAM (6 of 6), bretylium (3 of 3), and verapamil (3 of 3) all converted aconitine-induced VF to VT (Fig. 4). The VT rates after conversion were 9.7, 7.3, and 14.1 Hz, respectively ($P < 0.01$). The time intervals between drug infusion and conversion of VF to VT were 12.3 ± 5.1, 13 ± 5.2, and 24.3 ± 4.0 min, respectively. Verapamil conversion time was significantly longer compared with DAM and bretylium ($P < 0.05$).

All drug effects were reversible on washout, with VT converting back to VF within 8.5 ± 3.0, 6.3 ± 0.3, and 11.7 ± 1.5 min for DAM, bretylium, and verapamil, respectively (P = not significant). Figure 4 also shows typical examples. In these examples, DF did not change significantly with DAM or bretylium (Table 1). In contrast, DF increased significantly with verapamil ($P < 0.01$).

Table 1 summarizes DF at different stages of the experiments. When the baseline aconitine-induced VF of all nine RVs were pooled, the DF at the aconitine injection site was significantly higher than the DF registered by the pseudo-ECG (10.1 ± 1.6 vs. 8.1 ± 1.6 Hz, respectively, $P < 0.05$). In all RVs, the maximal DF of the entire RV was located at the aconitine site. These results suggest that the aconitine site is a fixed and known origin for rapid focal activation during VF.

Thus, despite their very different electrophysiological profiles, all three APD restitution-flattening drugs converted VF to VT, with no clear relationship between their effects on DF and their ability to convert VF.

Fibrillatory conduction block and maintenance of aconitine-induced VF. We then examined whether VF could be maintained by passive fibrillatory conduction block driven by the aconitine site as the only mechanism of new wave break. In one RV, we gave bretylium to convert VF to VT and then reinjected the aconitine site with fresh aconitine (Fig. 5). With conversion to VT by bretylium, DF decreased to 6.6 Hz. Reinjection of aconitine then increased DF at the aconitine site to 15.8 Hz, causing 2:1 conduction block (7.9 Hz) at distance sites. The pseudo-ECG and optical traces continued to show VT under these conditions, and electrocardiographic VF never occurred. The addition of verapamil to shorten refractoriness (while retaining flat APD restitution) allowed the resumption of 1:1 conduction at the high frequency (14.6 Hz) of the aconitine site, with the electrogram still showing VT but at a faster rate. Thus, with flat APD restitution, the rapid focal discharge (VT) did not undergo fibrillatory conduction and no VF was induced.

In two RVs, we excised the aconitine site after VT-to-VF transition had occurred. DF on the pseudo-ECG before and after excision were the same, and VF persisted for >15 min. These findings are similar to those

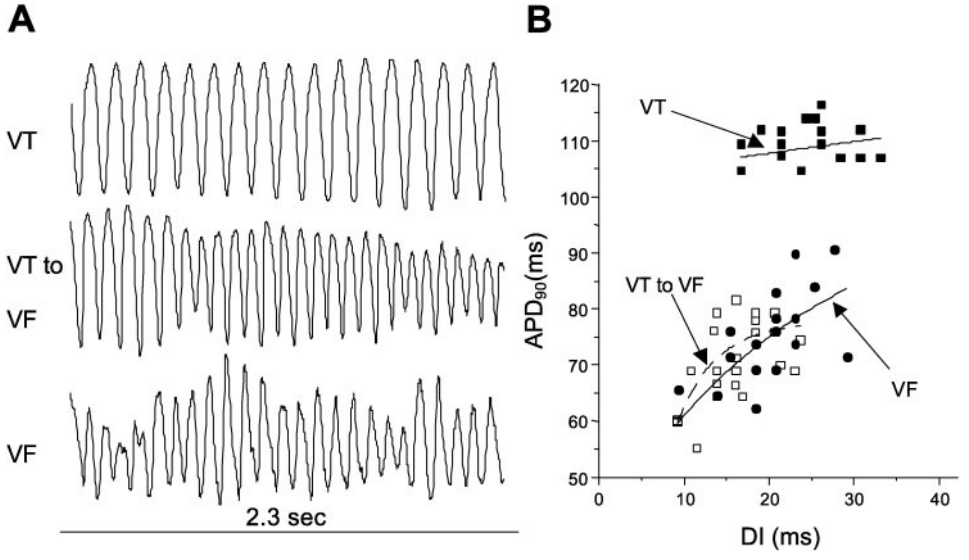

Fig. 3. Action potential duration (APD) restitution during, before and after VT-to-VF transition. *A*: representative optical recordings of aconitine-induced VT, VT-to-VF transition, and VF in the same RV. Note that there was a slight variation of VT CL (128–122 ms). APD ranged between 103 and 110 ms and the depolarization interval (DI) ranged between 16 and 29 ms. *B*: APD restitution curves during VT (■), VT-to-VF transition (□), and VF (●). The maximal slope of APD restitution curves for VT, VT to VF, and VF were 0.226, 3.3, and 1.76, respectively. APD_{90}, APD at 90% repolarization.

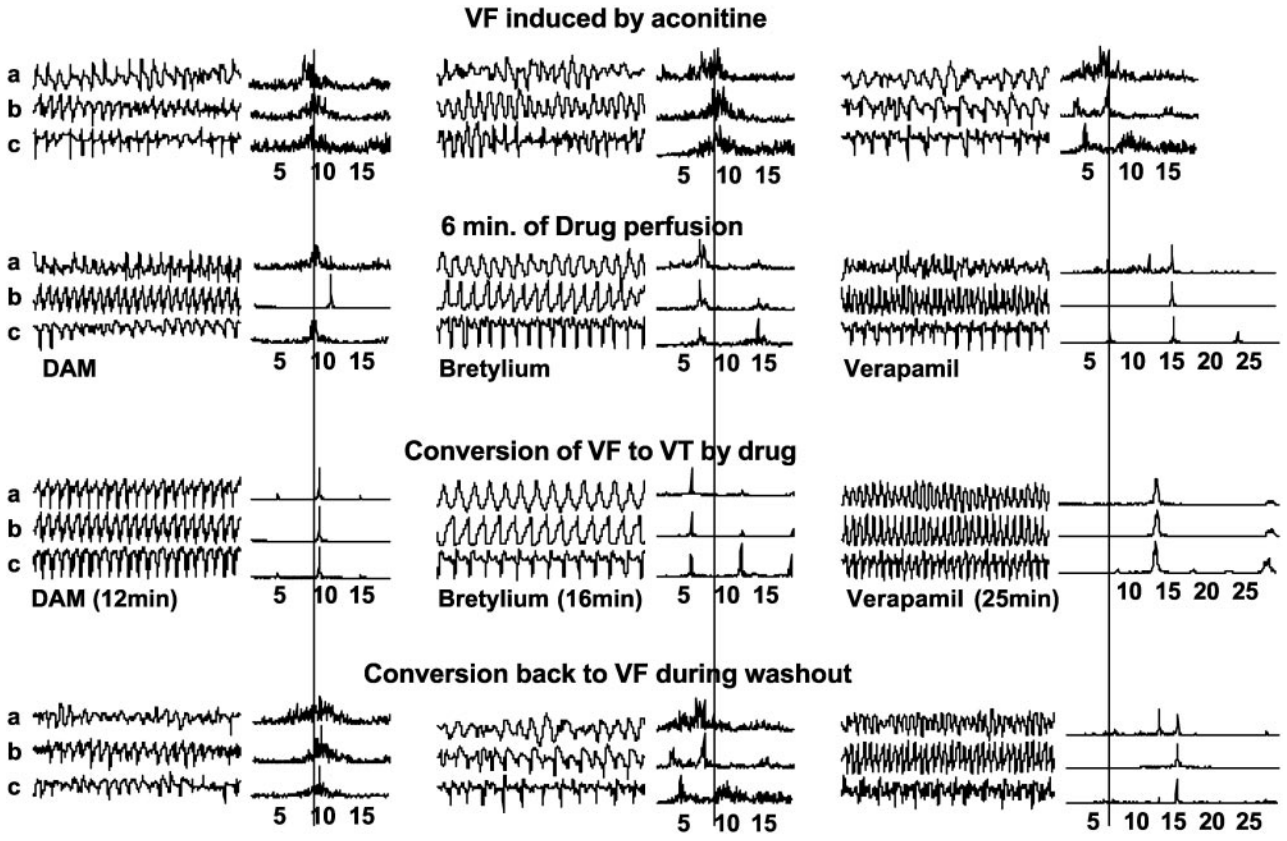

Fig. 4. DF analysis of the ECG recordings obtained during various phases of the study. *Left* to *right*: recordings associated with diacetyl monoxime (DAM), bretylium, and verapamil experiments, respectively. A vertical line was drawn through the DF of baseline VF. There was no change of DF with DAM, a small but insignifcant reduction of DF with bretylium, and significant increase of DF with verapamil. See text for details.

found in aconitine-induced atrial fibrillation. Once induced, the atrial fibrillation is also independent of the aconitine focus (14).

Computer simulations. To gain further insight into the role of APD restitution in focal source VF, we performed computer simulations using a modified version of the Luo-Rudy phase 1 ventricular AP model in simulated two-dimensional cardiac tissue incorporating a physiological degree of APD dispersion (see METHODS). We stimulated the effects of aconitine by pacing a small region (the "aconitine focus") in the center of the tissue (*site 2* of Fig. 6*A*) whenever the diastolic interval exceeded a critical (adjustable) duration. Under control conditions, in which the APD restitution slope was steep enough (>1) to produce spontaneous spiral wave breakup, increasing the frequency of the aconitine focus >9 Hz led to a distant wave break, which initiated "VF" (Fig. 6*D*). At this point, a second higher-frequency component at 10.8 Hz appeared due to penetration of the aconitine focus by outside reentrant wave fronts (Fig. 6*B*), reproducing the experimental observations in Fig. 2*B*. As in Fig. 2*B*, the FFT spectra for the transition from VT to VF shows two peaks, at 9.1 and 10.4 Hz. The first is attributable exclusively to the VT

Table 1. *Dominant frequency analysis*

Group	*n*	Aconitine-Induced VF, Hz	6 Min of Drug Perfusion, Hz	VF-to-VT Conversion, Hz	VF After Washout, Hz	*P*
DAM	6					
Pseudo-ECG		8.1 ± 1.6	9.4 ± 1.4	9.7 ± 1.2	10.9 ± 0.4 Hz	NS
Aconitine site		10.1 ± 1.8	10.3 ± 1.4	9.7 ± 1.2	11.1 ± 0.4 Hz	NS
Bretylium	3					
Pseudo-ECG		7.5 ± 2.2	7.6 ± 0.4	7.3 ± 0.2	8.3 ± 0.9	NS
Aconitine site		8.8 ± 1.6	7.6 ± 0.4	7.3 ± 0.2	8.2 ± 0.9	NS
Verapamil	3					
Pseudo-ECG		8.2 ± 0.9[1]	15.4 ± 1.0[2]	15.3 ± 0.8[3]	14.4 ± 0.5[4]	<0.01*
Aconitine site		8.2 ± 0.9[1]	14.8 ± 0.7[2]	14.0 ± 1.2[3]	14.4 ± 0.6[4]	<0.01*

Values are means ± SD; *n*, no. of pigs. VF, ventricular fibrillation; DAM, diacetyl monoxime; ECG, electrocardiogram; NS, not significant; VT, ventricular tachycardia. *Comparing 1 with 2, 3, and 4.

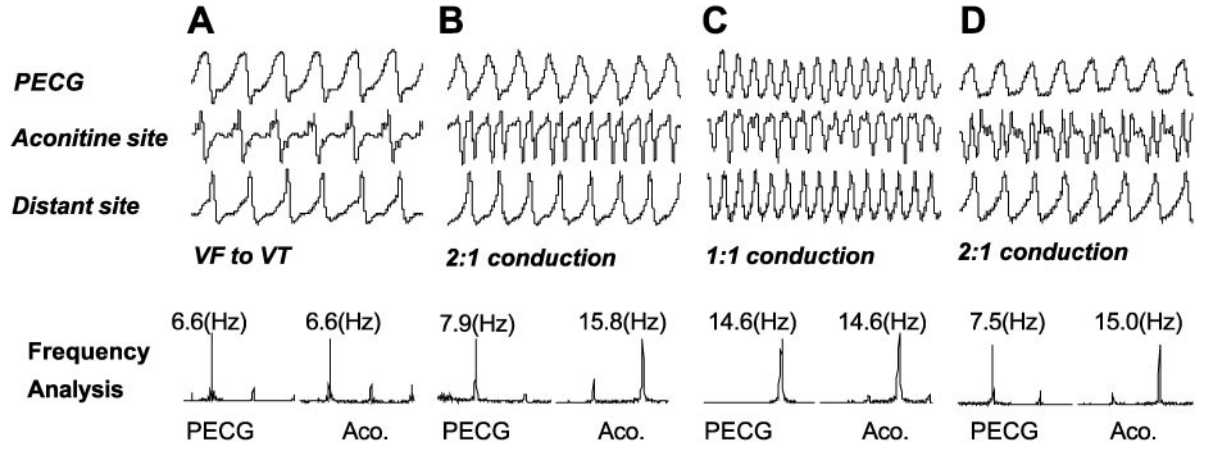

Fig. 5. Effects of combined bretylium and verapamil infusion. *A*: aconitine-induced VF was converted to VT by bretylium, with DF of 6.6 Hz (the VT DF on immediate transition was 7.2 Hz). *B*: local reinjection of aconitine increased the activation rate at aconitine site to 15.8 Hz with 2:1 conduction to the rest tissue. *C*: verapamil promoted 1:1 conduction with a frequency of 14.6 Hz. *D*: washout returned the tissue to 2:1 conduction with aconitine site activating at 15 Hz and the rest tissue at 7.5 Hz. PECG, DF of the pseudo-ECG; Aco, DF at the aconitine site.

phase immediately before VF, and the second is exclusively to the VF phase, as shown by the individual FFT spectra for the two phases. Figure 6*C* shows that the FFT spectra were qualitatively very similar to the FFT spectra for real data (Fig. 4). VF was self-sustaining and not dependent on the aconitine focus under these conditions because VF continued indefinitely when the focus was turned off.

If APD restitution slope in the Luo-Rudy phase 1 model was flattened to <1, increasing the frequency of

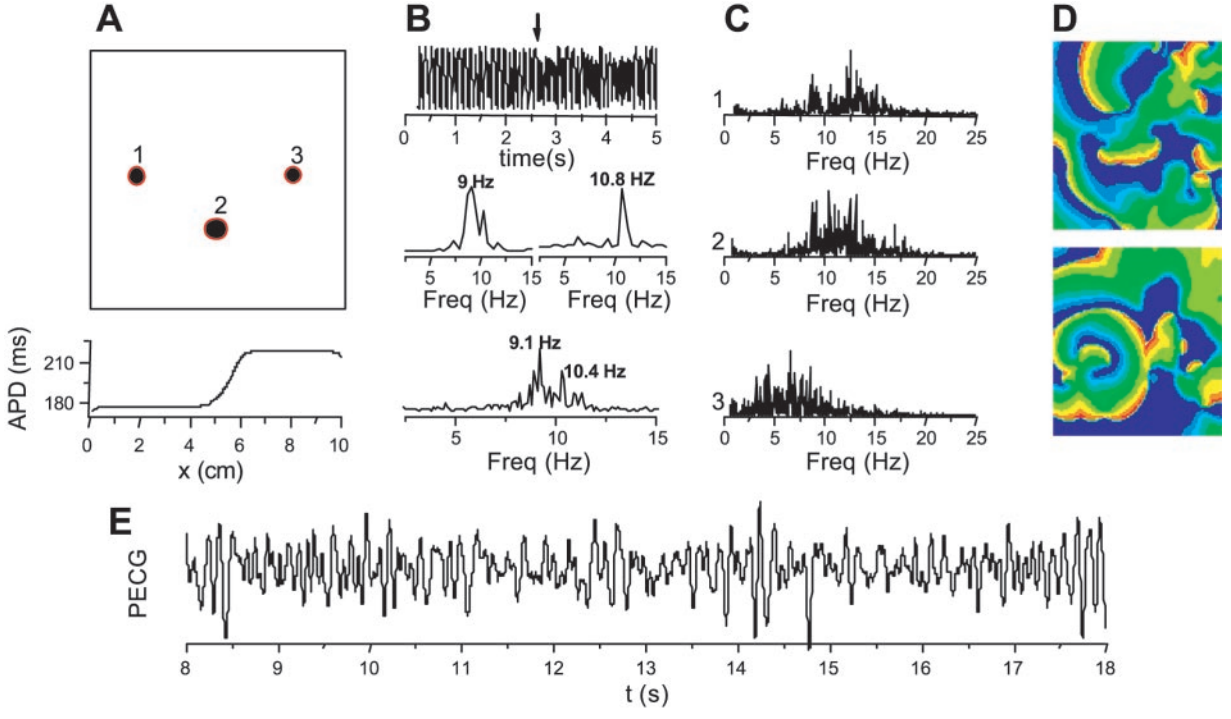

Fig. 6. Simulation of focal source VF associated with steep APD restitution [with maximum calcium channel conductance ($\bar{G}_{si}$) = 0.045 mS/cm^2 in the Luo-Rudy model, and α = 1.7 and β = 0.7 in *Eq. 2*]. *A*, *top*: locations of recording (1–3) and pacing sites (2) used to mimic the effects of aconitine (see METHODS). *Bottom*, APD distribution along the *x*-axis during pacing at 1,000 ms. *B*, *top*: intracellular membrane potential at *site 2* ("aconitine focus") during the transition from VT to VF (at arrow). *Middle*, FFT spectra for the final 2.5 s of VT (*left*) and the first 2.5 s of VF (*right*), illustrating the sudden increase in DF peak. *Bottom*, FFT spectrum for the full 5 s, showing two dominant peaks. *C*: FFT spectra from recording *sites 1–3* during a 20-s simulation after the onset of VF, showing broadband FFT spectra similar to those from the real heart (Fig. 4). *D*: two photos at *time 15 s* and *time 15.5 s* after the onset of VF, showing multiple wavelets. Voltage decreases from red (upstroke) to green (plateau) to blue (repolarized). *E*: PECG after VT-to-VF conversion.

the aconitine focus still led to wave break due to the APD heterogeneity in the tissue (Fig. 7, *A–F*). The broken waves then formed relatively stationary spiral waves in different domains of the tissue, with relatively narrow peaks in the FFT spectra corresponding to the intrinsic frequencies of these spiral waves. This divided the tissue into spatially discrete, relatively stationary domains each characterized by its own DF, similar to the experimental findings by Samie et al. (20). The pseudo-ECG continued to show VF (Fig. 7*B*, *bottom trace*), unlike the experimental results with APD restitution-flattening drugs, which converted VF to VT. However, as in the steep APD restitution case, once wave break occurred, maintenance of VF was not dependent on continued excitation from the aconitine focus, because it continued when the focus was turned off. Thus conduction block arising from rapid firing of the aconitine focus was essential for VF initiation, but its maintenance depended on the intrinsic spiral wave dynamics and not excitations from the focal source. If

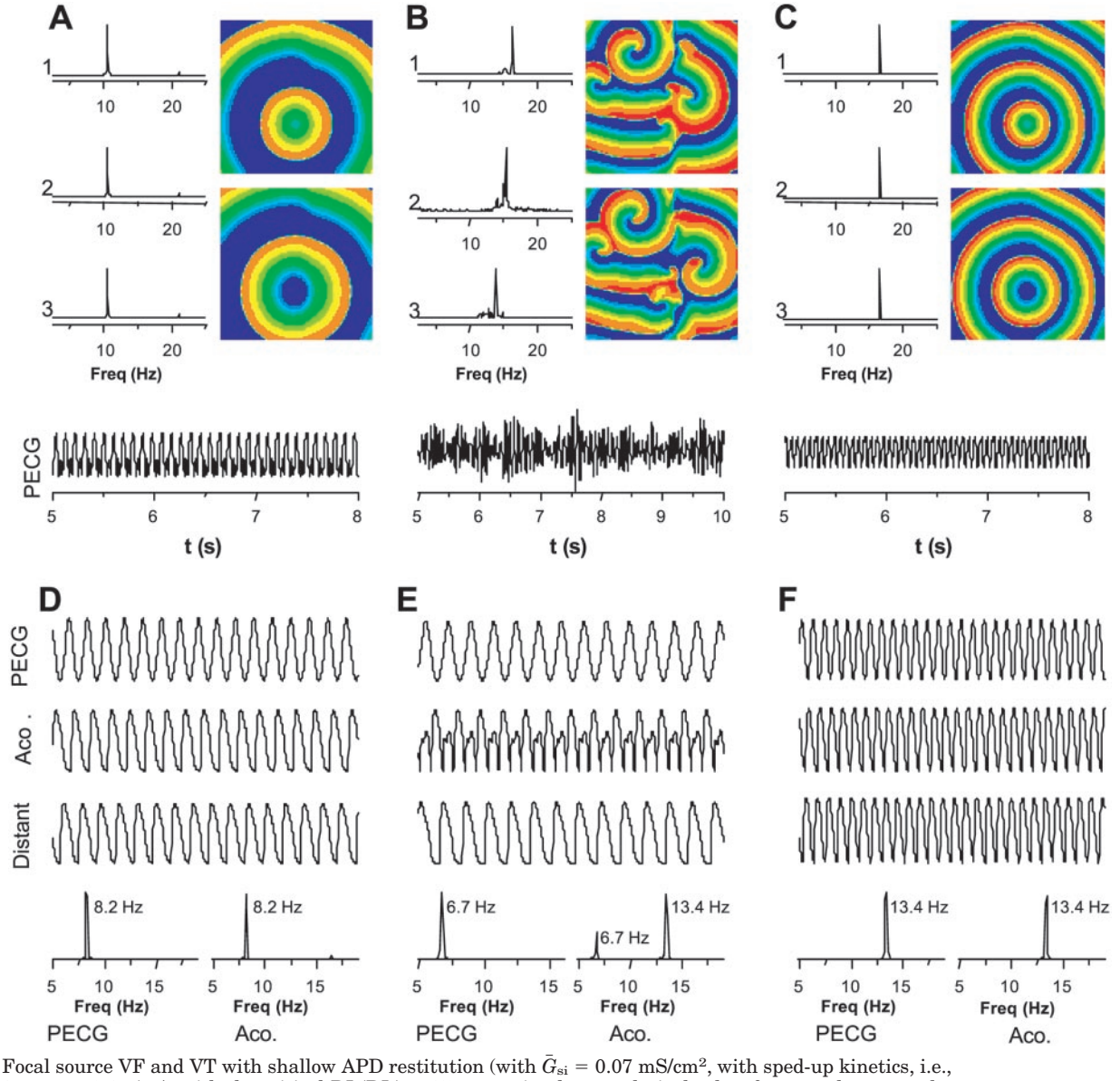

Fig. 7. Focal source VF and VT with shallow APD restitution (with $\bar{G}_{si}$ = 0.07 mS/cm^2, with sped-up kinetics, i.e., $\tau_d \rightarrow 0.1\ \tau_d$, $\tau_f \rightarrow 0.1\ \tau_f$). *A*: with the critical DI (DI$_c$) = 35 ms to simulate a relatively slow focus analogous to the postbretylium condition in Fig. 5*A*, FFT spectra from recording *sites 1–3* all showed a unique frequency of 10.5 Hz, and two photos at 9.5 and 10 s show that no wave break occurred. *B*: on shortening DI$_c$ to 10 ms to increase pacing rate (simulating aconitine reinjection in Fig. 5*B*), wave break occurred, leading to spiral wave reentry (*right*). FFT spectra at *sites 1–3* remained narrow, with each site showing different DFs (16.4, 15.4, and 13.8 Hz, respectively). *C*: With DI$_c$ = 15 ms, $\bar{G}_{si}$ was reduced to 0.04 mS/cm^2 to mimic the APD shortening effect of verapamil in Fig. 5*C*. No wave break occurred (*right*) and FFT spectra again showed a narrow spike at 16.7 Hz. With the use of the heterogeneity described in *Eq. 3* to ensure that the "acontine focus" remains faster than intrinsic spiral wave frequency, the results of Fig. 5, *A–C*, have been replicated. *D*: 1:1 conduction with DI$_c$ = 50 ms, simulating bretylium. *E*: 2:1 conduction with DI$_c$ = 10 ms, simulating reinjection of aconitine. *F*: 1:1 conduction restored by reducing $\bar{G}_{si}$ to 0.04 mS/cm^2 to simulate verapamil.

APD was shortened further throughout the tissue, 1:1 conduction could be maintained without wave break and spiral wave formation (Fig. 7*C*).

To reproduce the experimental findings in which APD restitution-flattening drugs converted VF to VT (Fig. 4) required that the aconitine focus have a higher frequency than the intrinsic frequency of any spiral waves in the tissue, to guarantee that the aconitine focus would always overdrive any spiral waves. This was achieved in the simulation by shortening the APD locally at the aconitine focus (Fig. 7, *D* and *E*). In this case, the rate of the aconitine focus, relative to the APD in the surrounding tissue, determined whether the tissue responded with 1:1 conduction (Fig. 7, *D* and *F*, corresponding to Fig. 5, *A–D*) or 2:1 conduction (Fig. 7*E*, corresponding to Fig. 5*B*). In all three cases, the pseudo-ECG showed monomorphic VT, consistent with the experimental findings.

DISCUSSION

There are three major findings: *1*) aconitine-induced rapid focal discharges and sustained VT; *2*) at baseline, spontaneous VT-to-VF transitions occurred due to the creation of new wave breaks; and *3*) drugs that flattened APD restitution converted VF back to VT, despite continuous rapid activation from aconitine site.

Computer simulation studies. Computer simulations provided further insights into the mechanisms of VF. When electrocardiographic VF was present, VF was maintained by the intrinsic dynamics of the spiral waves in the tissue rather than by the aconitine focus with fibrillatory conduction block in the surrounding tissue. Under these conditions, APD restitution steepness determined whether spatially discrete domains with a characteristic dominant frequency were stationary in time. When the intrinsic frequencies of spiral waves in the tissue were lower than the frequency of the aconitine focus, VF invariably converted to VT, whether conduction block was present or not. These findings indicate that APD restitution characteristics play a major role in determining the "phenotype" of VF.

Aconitine-induced VT-to-VF ratio. A key finding is that with the onset of VF, DF at the aconitine site suddenly jumped to a higher value, indicating that the aconitine injection site was being penetrated repeatedly by outside wave fronts. Thus, when conduction block at distant sites produced VF, wave breaks generated at these sites created rotors with higher frequencies than the aconitine focus. Once VF was initiated, the aconitine focus was no longer required for its maintenance.

Mechanisms of VF-to-VT transition. If the focal source hypothesis of VF is correct, two mechanisms by which a drug might be predicted to convert VT to VF by eliminating fibrillatory conduction block are *1*) by decreasing the frequency of the focal source to allow 1:1 capture or *2*) by decreasing the refractory period of the tissue to allow 1:1 capture at the same focal source frequency. Samie et al. (20) proposed that verapamil converted VF to VT by both mechanisms. However, Chorro et al. (2) found that DF did not correlate with activation patterns in VF. Rather, verapamil increased DF, whereas flecainide and sotalol diminished DF. Despite the divergent effects, all three drugs reduced the complexity of activation patterns in VF. Riccio et al. (19) showed that verapamil initially increased DF but increased VF organization in isolated canine ventricles. It eventually converted VF to VT without significantly altering DF over that during control VF. These results are inconsistent with the DF hypothesis (20).

An alternative mechanism to explain VF to VT transition by antiarrhythmic drugs is through flattening APD restitution (3, 19). DAM, verapamil, and bretylium all converted aconitine-induced focal source VF to VT, and all three drugs flatten APD restitution. In addition, DAM and verapamil decrease APD during both pacing and VF (11). Because decreased APD can facilitate 1:1 conduction and might therefore convert focal source VF to VT by eliminating fibrillatory conduction block, we also tested bretylium, which significantly increases APD (3). It also converted VF to VT. To rule out that the effects of bretylium were primarily mediated by slowing the aconitine focus, thereby eliminating fibrillatory conduction block, we reinjected aconitine in one experiment, which accelerated its rate sufficiently to induce conduction block away from the focus. Yet the rhythm remained periodic as VT, and electrocardiographic VF did not occur. Thus, all three APD restitution-flattening drugs converted VF to VT, independent of their effects on APD and refractory period. These findings support the restitution hypothesis of VF.

Limitation of the study. To minimize the physiological effects of an electromechanical uncoupler on the patterns of activation in VF, we chose not to use an electromechanical uncoupler during baseline VF mapping studies. A limitation of optical mapping study is that cardiac contraction may result in significant motion artifact of the optical signals. This problem is most apparent during sinus or paced rhythm, when the ventricles contract vigorously. However, our previous studies (9) showed that the VF CLs and patterns of activation detected with the optical mapping system was the same with or without the electromechanical uncoupler cytochalasin D. These data suggest that in the swine RV, optical mapping of VF can be performed without the use of an electromechanical uncoupler.

We thank Ivan Velasquez, Avile McCullen, Meiling Yuan, Elaine Lebowitz, and Scott T. Lamp for assistance.

This study was performed during the tenure of Fellowship grants from the Save a Heart Foundation and the Israel Pacing Foundation (to M. Swissa), College of Medicine, Yonsei University, Seoul, Korea, and the Myung Sun Kim Memorial Foundation (both to M.-H. Lee). This study was also supported in part by National Heart, Lung, and Blood Institute Grants P50-HL-52319 and R01-HL-66389, American Heart Association (AHA) National Center Grant-in-Aid 9750623N and 9950464N, AHA National Center Scientist Development Grant 0130171N, Cedars-Sinai Electrocardiographic Heart Beat Organization Foundation Award UC-TRDRP 9RT-0041, the Kawata and Laubisch Endowments, a Pauline and Harold Price Endowment, and the Ralph M. Parsons Foundation (Los Angeles, CA).

REFERENCES

1. **Alferness C, Bayly PV, Krassowska W, Daubert JP, Smith WM, and Ideker RE.** Strength-interval curves in canine myocardium at very short cycle lengths. *Pacing Clin Electrophysiol* 17: 876–881, 1994.
2. **Chorro FJ, Canoves J, Guerrero J, Mainar L, Sanchis J, Such L, and Lopez-Merino V.** Alteration of ventricular fibrillation by flecainide, verapamil, and sotalol: an experimental study. *Circulation* 101: 1606–1615, 2000.
3. **Garfinkel A, Kim YH, Voroshilovsky O, Qu Z, Kil JR, Lee MH, Karagueuzian HS, Weiss JN, and Chen PS.** Preventing ventricular fibrillation by flattening cardiac restitution. *Proc Natl Acad Sci USA* 97: 6061–6066, 2000.
4. **Jalife J, Berenfeld O, Skanes A, and Mandapati R.** Mechanisms of atrial fibrillation: mother rotors or multiple daughter wavelets, or both? *J Cardiovasc Electrophysiol* 9: S2–S12, 1998.
5. **Karma A.** Electrical alternans and spiral wave breakup in cardiac tissue. *Chaos* 4: 461–472, 1994.
6. **KenKnight BH, Bayly PV, Gerstle RJ, Rollins DL, Wolf PD, Smith WM, and Ideker RE.** Regional capture of fibrillating ventricular myocardium: evidence of an excitable gap. *Circ Res* 77: 849–855, 1995.
7. **Kim YH, Garfinkel A, Ikeda T, Wu TJ, Athill CA, Weiss JN, Karagueuzian HS, and Chen PS.** Spatiotemporal complexity of ventricular fibrillation revealed by tissue mass reduction in isolated swine right ventricle. Further evidence for the quasiperiodic route to chaos hypothesis. *J Clin Invest* 100: 2486–2500, 1997.
8. **Kobayashi Y, Peters W, Khan SS, Mandel WJ, and Karagueuzian HS.** Cellular mechanisms of differential action potential duration restitution in canine ventricular muscle cells during single versus double premature stimuli. *Circulation* 86: 955–967, 1992.
9. **Lee MH, Lin SF, Ohara T, Omichi C, Okuyama Y, Chudin E, Garfinkel A, Weiss JN, Karagueuzian HS, and Chen PS.** Effects of diacetyl monoxime and cytochalasin D on ventricular fibrillation in swine right ventricles. *Am J Physiol Heart Circ Physiol* 280: H2689–H2696, 2001.
10. **Lin SF, Abbas RA, and Wikswo JP Jr.** High-resolution high-speed synchronous epifluorescence imaging of cardiac activation. *Rev Sci Instrum* 68: 213–217, 1997.
11. **Liu Y, Cabo C, Salomonsz R, Delmar M, Davidenko J, and Jalife J.** Effects of diacetyl monoxime on the electrical properties of sheep and guinea pig ventricular muscle. *Cardiovasc Res* 27: 1991–1997, 1993.
12. **Luo CH and Rudy Y.** A model of the ventricular cardiac action potential. Depolarization, repolarization, and their interaction. *Circ Res* 68: 1501–1526, 1991.
13. **Moe GK.** On the multiple wavelet hypothesis of atrial fibrillation. *Arch Int Pharmacodyn Ther* 140: 183–188, 1962.
14. **Moe GK and Abildskov JA.** Atrial fibrillation as a self-sustaining arrhythmia independent of focal discharge. *Am Heart J* 58: 59–70, 1959.
15. **Nolasco JB and Dahlen RW.** A graphic method for the study of alternation in cardiac action potentials. *J Appl Physiol* 25: 191–196, 1968.
16. **Prinzmetal M, Corday E, Brill IC, Sellers AL, Oblath RW, Flieg WA, and Kruger HE.** Mechanism of the auricular arrhythmias. *Circulation* 1: 241–245, 1950.
17. **Qu Z, Garfinkel A, Chen PS, and Weiss JN.** Mechanisms of discordant alternans and induction of reentry in simulated cardiac tissue. *Circulation* 102: 1664–1670, 2000.
18. **Qu Z, Weiss JN, and Garfinkel A.** Cardiac electrical restitution properties and stability of reentrant spiral waves: a simulation study. *Am J Physiol Heart Circ Physiol* 276: H269–H283, 1999.
19. **Riccio ML, Koller ML, and Gilmour RFJ.** Electrical restitution and spatiotemporal organization during ventricular fibrillation. *Circ Res* 84: 955–963, 1999.
20. **Samie FH, Mandapati R, Gray RA, Watanabe Y, Zuur C, Beaumont J, and Jalife J.** A mechanism of transition from ventricular fibrillation to tachycardia: effect of calcium channel blockade on the dynamics of rotating waves. *Circ Res* 86: 684–691, 2000.
21. **Voroshilovsky O, Qu Z, Lee MH, Ohara T, Fishbein GA, Huang HL, Swerdlow CD, Lin SF, Garfinkel A, Weiss JN, Karagueuzian HS, and Chen PS.** Mechanisms of ventricular fibrillation induction by 60-Hz alternating current in isolated swine right ventricle. *Circulation* 102: 1569–1574, 2000.
22. **Weiss JN, Garfinkel A, Karagueuzian HS, Qu Z, and Chen PS.** Chaos and the transition to ventricular fibrillation: a new approach to antiarrhythmic drug evaluation. *Circulation* 99: 2819–2826, 1999.
23. **Zaitsev AV, Berenfeld O, Mironov SF, Jalife J, and Pertsov AM.** Distribution of excitation frequencies on the epicardial and endocardial surfaces of fibrillating ventricular wall of the sheep heart. *Circ Res* 86: 408–417, 2000.